Well-Ordered Microdomain Structures in Polydisperse Poly(styrene)−Poly(acrylic acid) Diblock Copolymers from Controlled Radical Polymerization

D. Bendejacq, V. Ponsinet,* and M. Joanicot

Complex Fluids Laboratory, UMR 166 CNRS/Rhodia, Cranbury, New Jersey 08512

Y.-L. Loo[†,§] and R. A. Register[‡]

Department of Chemical Engineering and Princeton Materials Institute, Princeton University, Princeton, New Jersey 08544

Received January 30, 2002

ABSTRACT: To investigate whether diblock copolymers with substantial distributions of molecular weight and composition can self-assemble into highly regular microdomain structures, we examine the morphologies of polystyrene-*b*-poly(acrylic acid), diblock copolymers (PS−PAA) synthesized by controlled radical polymerization in emulsion. Despite diblock polydispersity indices of ca. 2, solvent-cast films of these diblocks, as well as their blends with PS homopolymer of low molecular weight, exhibit well-ordered lamellar or hexagonally packed cylindrical morphologies in the midrange of composition, as shown by small-angle X-ray scattering and transmission electron microscopy. In several specimens, well-ordered regions of lamellae and cylinders appear to coexist. Films of very asymmetric diblocks or blends exhibit spherical microdomains without lattice order.

Introduction

The self-assembly of block copolymers in bulk has been extensively described, both theoretically and experimentally, over the past few decades.[1] The presence or absence of microphase separation depends on the segregation strength between the blocks, while the morphology of the microphase-separated structure (when present) is governed principally by the volume ratio of the blocks, modulated weakly by the segregation strength[2] and the conformational asymmetry[3] of the diblock.

Theories for monodisperse block copolymers[2] indicate that the ordered phases should consist of regular packings of microdomains, including the body-centered-cubic packing of spheres, hexagonally packed cylinders (denoted C below), and alternating lamellae (L). Most experimental studies of phase behavior have employed block copolymers prepared by "living" anionic polymerization, which typically yields polydispersity indices (PI $\equiv M_w/M_n$, the ratio of weight- to number-average molecular weights) less than 1.1 and with negligible compositional heterogeneity between chains, thus approaching the monodisperse limit. Well-annealed films of such block copolymers typically *do* exhibit lattice order, as evidenced by a series of peaks in the small-angle X-ray scattering (SAXS) pattern corresponding to the lattice's structure factor. Cases where lattice order is not observed in near-monodisperse block copolymers appear to reflect kinetic limitations in reaching the equilibrium morphology.[4]

To rapidly map the phase diagram for diblocks of a particular chemistry, diblocks are often blended with low-molecular-weight homopolymer of one of the blocks,[5,6] or with each other.[3,7,8] This approach generally produces well-ordered morphologies, provided that the homopolymer molecular weight is sufficiently low or that the diblocks are sufficiently well-matched in composition and molecular weight. Such bidisperse blends have been treated theoretically,[9−13] and agreement between theory and experiment is at least qualitatively good. By contrast, very little is known about the phase behavior of amorphous diblocks possessing *continuous* distributions of composition and/or molecular weight. Segmented copolymers such as polyurethanes, where at least one type of segment has a polydispersity of ca. 2, do not exhibit well-ordered microdomains even when the segregation strength is large and the polymer is nearly symmetric,[14] suggesting that polydispersity may substantially reduce the microdomain order.

The development of controlled radical polymerization (CRP) over the past decade[15−18] has greatly expanded the range of monomers that can be incorporated into diblock architectures. While polydispersities as low as those characteristic of anionic polymerization are obtainable in some cases, in general polymers produced by CRP are substantially more polydisperse. This raises anew the question of the phase behavior and microdomain order of polydisperse diblocks. Potential applications where good microdomain lattice order is required include the formulation of soft solids with controllable modulus[19,20] and yield stress,[20] and templates for regular arrays of nanostructures.[21−23] The chemical diversity and functionality offered by CRP are especially attractive for these applications, provided good lattice order can be achieved. While Leclère and co-workers[24] demonstrated regular microdomain order in thin films of CRP-derived acrylate triblocks with PI $\leq$ 1.3, Li and co-workers[25] found only an irregular microdomain structure in a polystyrene−polyisoprene−polystyrene triblock with PI = 1.6.

[†] Department of Chemical Engineering.
[‡] Princeton Materials Institute.
[§] Permanent address: Chemical Engineering Dept., The University of Texas at Austin, Austin TX 78712.
* Author for correspondence: e-mail Virginie.Ponsinet@us.rhodia.com.

10.1021/ma020158z CCC: $22.00
Published on Web 07/10/2002

Table 1. Compositions, Molecular Weights, and Polydispersities of the Pure Diblocks

sample code	PS weight fraction (w_{PS})	PS block M_n (g mol^{-1})	PS block PI[a]	diblock M_n (g mol^{-1})[b]	diblock PI[a]
(12)	0.120	2040	2.00	17 000	2.10
(19)	0.186	3140	1.83	16 900	2.41
(27)	0.271	4560	1.77	16 800	2.61
(48)	0.481	8700	2.16	18 100	2.18
(51)	0.513	2070	2.31	4 040	2.20
(88)	0.884	13000	2.21	14 700	2.13

[a] Polydispersity index PI $\equiv M_w/M_n$, as obtained on the unhydrolyzed precursor by GPC calibrated with narrow-distribution PS standards. For the diblock, the apparent PI quoted here is an approximation to the true PI. [b] Total molecular weight of the diblock, computed as the ratio of column 3 to column 2.

Table 2. Compositions and Structures of Pure Diblocks and Blends

sample code	composition[a]	PS weight fraction (w_{PS})	PS vol fraction[b] (ϕ_{PS})	interdomain spacing d (nm)	morphology[c]
(12)	neat (12)	0.120	0.16	23.0	nl
(19)	neat (19)	0.186	0.24	24.1	nl
(27-A-26)	(27) + 5% PAA	0.257	0.33	26.3	nl
(19-S-27)	(19) + 10% PS	0.267	0.34	31.7	C
(27)	neat (27)	0.271	0.34	25.6	C
(27-S-29)	(27) + 2.5% PS	0.289	0.36	27.0	C
(27-S-31)	(27) + 5% PS	0.308	0.38	30.6	C (+ L)
(27-S-34)	(27) + 10% PS	0.343	0.42	32.6	L (+ C)
(48)	neat (48)	0.481	0.56	34.0	L
(51)	neat (51)	0.513	0.60	16.4	L
(48-S-58)	(48) + 20% PS	0.584	0.66	44.6	L
(48-S-64)	(48) + 30% PS	0.638	0.71	46.5	L (+ C)
(48-S-70)	(48) + 40% PS	0.704	0.77	50.7	C
(88)	neat (88)	0.884	0.91	34.9	nl

[a] Homopolymer content expressed as a weight percentage of the sample. [b] Calculated with the mass density values d = 1.47 and 1.05 g cm^{-3} respectively for PAA (see text) and PS. [c] nl = no well-defined lattice observed by SAXS; C = hexagonally packed cylinders; L = alternating lamellae. Entries in parentheses indicate the minor structure when two coexisting structures are present.

A novel CRP technique, termed "macromolecular design by interchange of xanthate" (MADIX), has been developed by Rhodia.[26−28] This transfer-agent-mediated reaction permits easy synthesis of a broad range of block copolymers, including those with acrylate blocks. Hydrolysis to poly(acrylic acid) provides a facile route to amphiphilic polyelectrolyte diblocks, whose phase behavior is of interest in both bulk and solution. Here, we investigate the morphology of solvent-cast films of MADIX-derived polystyrene-*b*-poly(acrylic acid) diblock copolymers (PS−PAA) and blends of these diblocks with PS or PAA homopolymer of low molecular weight. To the best of our knowledge, this is the first systematic investigation of microdomain morphology as a function of composition for any CRP-derived diblock family.

Experimental Section

Diblock Synthesis and Characterization. Six polystyrene-*b*-poly(ethyl acrylate) diblock copolymers, PS−PEA Rhodiblocks, were synthesized by MADIX[26−28] in aqueous emulsion. The concentrations of polymer latexes were close to 30% (w/w) at the end of the synthesis. In all cases, the PEA block contains 2−5 wt % methacrylic acid comonomer. The molecular weight and polydispersity of the PS first block (sampled prior to the addition of ethyl acrylate) and of the PS−PEA diblock were measured by gel permeation chromatography (GPC), using a series of Phenogel columns, tetrahydrofuran (THF) as eluent (1 mL/min), and a differential refractive index detector. The system was calibrated with narrow-distribution PS standards. The PS and PEA hydrodynamic volumes differ at fixed molecular weight, as do their refractive index increments in THF. Since the diblocks are found to exhibit compositional polydispersity, the PI values determined from their chromatograms are approximations to the true values.

The ethyl acrylate units were then hydrolyzed to sodium acrylate in a sealed glass reactor with NaOH (2 mol/mol of acrylate) for 24 h at 90−95 °C, at 4 wt % diblock. The solutions were then precipitated into aqueous HCl at pH 1, redispersed in water/THF, and extensively dialyzed against aqueous HCl (pH 2.5) to purify the polymers and convert the poly(acrylic acid) blocks completely to the acid form, rendering the diblocks fully soluble in THF. The polymers were finally isolated by freeze-drying.

^{1}H NMR spectroscopy (Oxford AS400 MHz) was performed in deuterated pyridine, yielding the hydrolysis efficiency (≥98%), along with the diblock compositions as presented in Table 1. Diblocks are represented by a two-digit sample code which equates to the weight percent PS in the diblock, e.g., (12) is a diblock containing 12 wt % PS.

Specimen Preparation. Films 0.2−0.4 mm thick were cast over 3−4 days from 15 to 20 wt % solutions in THF (a good solvent for both PS and PAA) in poly(tetrafluoroethylene) molds and then dried overnight under vacuum at room temperature and finally for an hour at 60 °C to remove traces of THF. Low molecular weight PS (M_n = 680 g mol^{-1}, PI = 1.12) and PAA (M_n = 1020 g mol^{-1}, PI = 1.73) homopolymers were purchased from Aldrich and used as received. These were blended with diblock in THF solution, and films were cast as described above. Blend compositions are indicated in Table 2. Blends are represented by a five-character sample code, indicating the diblock and homopolymer used and the weight fraction of polystyrene in the blend. For example, blend (19-S-27) is prepared from diblock (19), blended with PS homopolymer (S = PS, A = PAA) such that the blend contains a total of 27 wt % PS (counting both diblock and homopolymer PS).

Morphological Characterization. Small-angle X-ray scattering (SAXS) was used to identify the lattice types and spacings of the neat diblocks and blends, all at room temperature using the solvent-cast films described above. All SAXS profiles were acquired in transmission, using procedures described previously,[29] with Cu Kα radiation from a sealed-tube source collimated with a compact Kratky camera (Anton-Paar), and the scattering profiles acquired with a one-dimensional position-sensitive detector (Braun OED-50M). The angular axis is presented in $q = (4\pi/\lambda) \sin \theta$, where λ is the

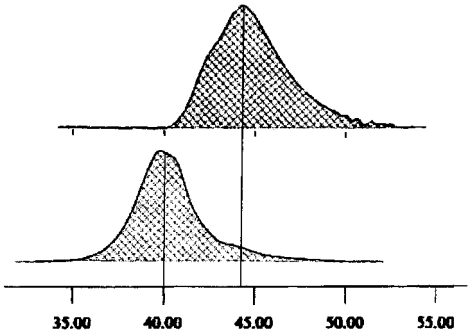

Figure 1. GPC curves for the PS first block (top) and the unhydrolyzed PS−PEA precursor (bottom) for diblock (12). Crosshatched regions correspond to those used for calculation of polydispersity index, PI.

wavelength of the Cu Kα radiation and θ is half the scattering angle. In the figure presented here, SAXS intensities for specimens exhibiting the L phase are multiplied through by q^2, while those for C phase specimens are multiplied through by q, as a first-order correction[30] for the impact of the form factor $P(q)$ of individual cylinders and lamellae on the observed scattering intensity $I(q)$. Thus, the peak positions in q^2I or qI correspond more closely to the peaks in the lattice's structure factor $S(q)$, from which the interdomain spacing d is extracted. For transmission electron microscopy (TEM), unstained films were embedded in epoxy and cured at 50 °C. Sections (100 nm) were obtained at room temperature with an Ultracut E ultramicrotome (Reichert-Jung) and were examined as such on a JEOL 1200 EX TEM at 120 kV.

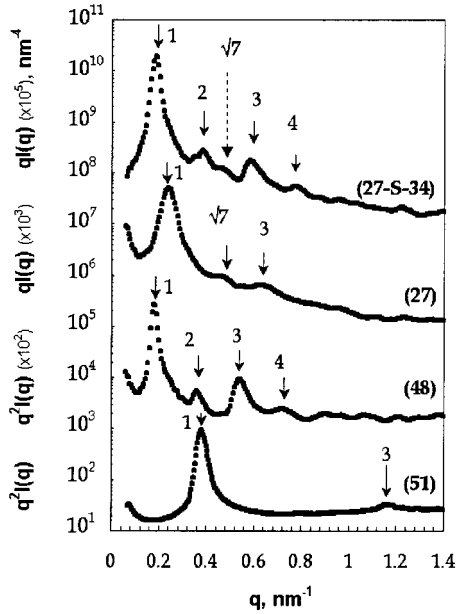

Figure 2. SAXS data (logarithmic intensity scale) for lamellar diblocks (52) and (48), cylinder-forming diblock (27), and the blend (27-S-34), from bottom to top. Downward-pointing arrows indicate the positions of lattice structure factor peaks, revealing the regular arrangement of the microdomains. Full-line and dotted-line arrows for the pattern of (27-S-34) respectively indicate lamellar and hexagonal lattice structure factor peaks.

Results and Discussion

Figure 1 presents the GPC traces for the unhydrolyzed polystyrene-*b*-poly(ethyl acrylate) precursor (PS−PEA) to diblock (12) and its corresponding PS block (first block). The first block exhibits a broad peak centered at an elution time of ca. 44 min, while the diblock exhibits a main peak centered at 40 min along with a small shoulder at 44 min, reflecting terminated first block. Both the first block and the diblock have PI ≈ 2, as detailed in Table 1.

Lattice Order in Lamella- and Cylinder-Forming Diblocks. The most striking result of this work is shown in Figure 2, which presents SAXS patterns for four systems showing well-ordered microdomain structures despite the substantial polydispersity. The lower two curves correspond to two near-symmetric diblocks of very different molecular weights: diblock (48) shows sharp peaks at q ratios of 1:2:3:4, while the lower-M_n diblock (51) shows peaks at q ratios of 1:2:3. For both lamellar diblocks, the intensities of the even-order reflections are weaker than those of the odd-order reflections. Analysis of the relative intensities of the even-order peaks in the SAXS patterns yields a density of 1.47 g cm^{-3} for PAA, in agreement with the value obtained by extrapolation of the densities of aqueous solutions[31] and which we use throughout to calculate the volume fraction of PS in the diblock (ϕ_{PS}) from the known w_{PS}.

The third curve in Figure 2 shows the SAXS pattern for a diblock with a PS weight fraction $w_{PS} = 0.27$, which exhibits peaks at q ratios of 1:$\sqrt{4}$:$\sqrt{7}$:$\sqrt{9}$, as expected for a well-ordered array of hexagonally packed cylinders. (The $\sqrt{3}$ peak is absent here due to the proximity of the cylinder form factor node.[32]) Values of the interdomain spacing d were calculated from the position of the first-order peak q^* as $d = 2\pi/q^*$ and are listed in Table 2. For lamellar specimens, d corresponds to the fundamental lamellar spacing, while for cylindrical specimens, d corresponds to the spacing between (10) planes in the hexagonal lattice. Polarized light microscopy shows that cast films of all three samples exhibit strong birefringence, as expected for cylinders and lamellae.

The unhydrolyzed PS−PEA precursors to these diblocks showed no microphase separation by SAXS, due to the small interaction parameter χ between PS and PEA.[33] However, the fact that diblock (51), with a small degree of polymerization (N), is ordered indicates that the Flory interaction parameter χ between PS and PAA is large. We use the fact that χN at the order−disorder transition, $(\chi N)_{ODT}$, equals 10.5 for symmetric diblock copolymers (in the mean-field limit[1,2]) to estimate $\chi > 0.3$, taking a styrene repeat unit as the reference volume. Since all the other diblocks have molecular weights approximately 4 times that of (51), they correspond to $\chi N > 50$, reflecting rather strong interblock segregation.

Morphologies of Asymmetric Diblocks and Blends. In contrast to the well-ordered C and L structures, materials with greater compositional asymmetry did not exhibit any lattice order. Diblocks (12), (19), and (88) exhibited SAXS patterns characteristic of a liquidlike packing of spheres[4,34] with a primary peak with high-q shoulder, followed at higher q by broad maxima characteristic of the form factor scattering from isolated spheres. It is unclear whether the absence of lattice order is an equilibrium consequence of the polydispersity or simply reflects kinetic limitations imposed by the solvent-casting process; highly asymmetric diblocks are more sluggish to order than their symmetric counterparts.[4] Unfortunately, the susceptibility of dry PAA to degradation and cross-linking at elevated temperatures precludes annealing these materials well above the PS glass transition temperature to push the morphologies toward equilibrium.

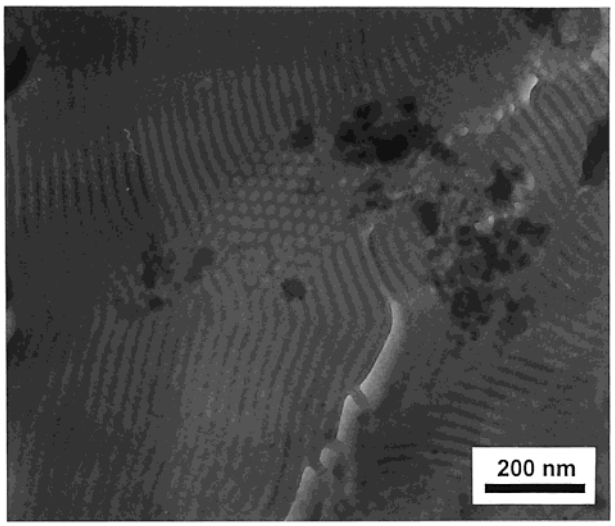

Figure 3. TEM image obtained on an unstained section of blend (27-S-34), showing large (1−2 μm) domains in which both structure and orientation are homogeneous. Large areas of long stripes are identified as lamellar domains, while the smaller domain of white dots in the center of the image indicates the presence of hexagonally packed cylinders. The values of the electron densities allow to identify the white areas as PS and the dark as PAA, and therefore the microstructure as a C phase comprising PS cylinders in a continuous PAA matrix.

Coexistence of Lamellae and Cylinders in Diblock−Homopolymer Blends. The addition of modest quantities of low-molecular-weight PS homopolymer to diblocks (27) and (48) induced morphological changes without a discernible effect on the degree of order exhibited by the microdomains. Between the C and the L phases, at $w_{PS} = 0.31$, 0.34 (shown as an example on the upper curve in Figure 2), and 0.64, the SAXS patterns present discernible $\sqrt{7}q^*$ reflections but also strong peaks at $2q^*$ and $4q^*$, therefore suggesting the presence of coexisting L and C mesophases, with similar values of q^*. That the q^* values should be similar is not surprising, as only small changes in q^* have been reported in other block copolymer systems during thermotropic L ↔ C transitions.[3,35]

We verified the L/C coexistence by performing transmission electron microscopy on a thin section of sample (27-S-34). The TEM image in Figure 3 shows grains of order 1 μm across, in which both microdomain structure and orientation are homogeneous. The majority of the image consists of well-ordered long stripes, which we identify with the majority L phase. Though stripes can also be presented by cylinders lying in the plane of the film, cylinders would be statistically unlikely to meander only in the plane of the image, as is the case in Figure 3. The smaller domain of hexagonally packed white dots in the center of the image clearly corresponds to the minority C phase.

Stable coexistence of two ordered phases is unexpected for monodisperse block copolymers and has not been conclusively shown in the literature for neat near-monodisperse diblocks in bulk. Typically,[3,6] the gyroid phase is found at compositions lying between C and L, but we did not detect any gyroid signature in our SAXS patterns. It is plausible, though speculative, that the polydispersity present in our systems somehow stabilizes coexisting L + C phases relative to a uniform gyroid (or L or C) phase. The coexistence could also results from the solvent-casting process, which can influence the final morphology.[36,37]

Acknowledgment. We are thankful to Annie Vacher and Marc Airiau, Rhodia, for TEM and to Mathias Destarac, Dominique Charmot, and Gilda Lizzaraga, Rhodia, for support in the synthesis. Y.-L.L. and R.A.R. gratefully acknowledge financial support from the National Science Foundation, Polymers Program (DMR-9711436), and the Princeton University Graduate School for the Porter Ogden Jacobus Honorific Fellowship (Y.-L.L.).

References and Notes

(1) Hamley, I. W. *The Physics of Block Copolymers*; Oxford University Press: New York, 1998.
(2) Matsen, M. W.; Bates, F. S. *Macromolecules* **1996**, *29*, 1091.
(3) Lai, C.; Russel, W. B.; Register, R. A.; Marchand, G. R.; Adamson, D. H. *Macromolecules* **2000**, *33*, 3461.
(4) Adams, J. L.; Quiram, D. J.; Graessley, W. W.; Register, R. A.; Marchand, G. R. *Macromolecules* **1996**, *29*, 2929.
(5) Winey, K. I.; Thomas, E. L.; Fetters, L. J. *Macromolecules* **1992**, *25*, 2645.
(6) Hadjuk, D. A.; Harper, P. E.; Gruner, S. M.; Honecker, C. C.; Kim, G.; Thomas, E. L.; Fetters, L. J. *Macromolecules* **1994**, *27*, 4063.
(7) Hashimoto, T.; Yamasaki, K.; Koizumi, S.; Hasegawa, H. *Macromolecules* **1993**, *26*, 2895.
(8) Zhao, J.; Majumdar, B.; Schulz, M. F.; Bates, F. S.; Almdal, K.; Mortensen, K.; Hajduk, D. A.; Gruner, S. M. *Macromolecules* **1996**, *29*, 1204.
(9) Matsen, M. W. *Macromolecules* **1995**, *28*, 5765.
(10) Whitmore, M. D.; Noolandi, J. *Macromolecules* **1985**, *18*, 2486.
(11) Lyatskaya, Yu. V.; Zhulina, E. B.; Birshtein, T. M. *Polymer* **1992**, *33*, 343.
(12) Spontak, R. J. *Macromolecules* **1994**, *27*, 6363.
(13) Matsen, M. W.; Bates, F. S. *Macromolecules* **1995**, *28*, 7298.
(14) Li, C.; Goodman, S. L.; Albrecht, R. M.; Cooper, S. L. *Macromolecules* **1988**, *21*, 2367.
(15) Matyjaszewski, K., Ed.; *Controlled Radical Polymerization*; ACS Symposium Series 685; American Chemical Society: Washington, DC, 1998.
(16) Matyjaszewski, K.; Xia, J. *Chem. Rev.* **2001**, *101*, 2921.
(17) Hawker, C. J.; Bosman, A. W.; Harth, E. *Chem. Rev.* **2001**, *101*, 3661.
(18) Kamigaito, M.; Ando, T.; Sawamoto, M. *Chem. Rev.* **2001**, *101*, 3689.
(19) Kossuth, M. B.; Morse, D. C.; Bates, F. S. *J. Rheol.* **1999**, *43*, 167.
(20) Sebastian, J. M.; Lai, C.; Graessley, W. W.; Register, R. A. *Macromolecules* **2002**, *35*, 2707.
(21) Park, M.; Chaikin, P. M.; Register, R. A.; Adamson, D. H. *Appl. Phys. Lett.* **2001**, *79*, 257.
(22) Li, R. R.; Dapkus, P. D.; Thompson, M. E.; Jeong, W. G.; Harrison, C.; Chaikin, P. M.; Register, R. A.; Adamson, D. H. *Appl. Phys. Lett.* **2000**, *76*, 1689.
(23) Thurn-Albrecht, T.; Schotter, J.; Kästle, G. A.; Emley, N.; Shibauchi, T.; Krusin-Elbaum, L.; Guarini, K.; Black, C. T.; Tuominen, M. T.; Russell, T. P. *Science* **2000**, *290*, 2126.
(24) Leclère, Ph.; Moineau, G.; Minet, M.; Dubois, Ph.; Jerome, R.; Brédas, J. L.; Lazzaroni, R. *Langmuir* **1999**, *15*, 3915.
(25) Li, I. Q.; Howell, B. A.; Dineen, M. T.; Kastl, P. E.; Lyons, J. W.; Meunier, D. M.; Smith, P. B.; Priddy, D. B. *Macromolecules* **1997**, *30*, 5195.
(26) Corpart, P.; Charmot, D.; Zard, S. Z.; Biadatti, T.; Michelet, D. US Patent 6,153,705, Nov 28, 2000, to Rhodia Chimie.
(27) Destarac, M.; Charmot, D.; Franck, X.; Zard, S. Z. *Macromol. Rapid Commun.* **2000**, *21*, 1035.
(28) Charmot, D.; Corpart, P.; Adam, H.; Zard, S. Z.; Biadatti, T.; Bouhadir, G. *Macromol. Symp.* **2000**, *150*, 23.
(29) Register, R. A.; Bell, T. R. *J. Polym. Sci., Part B: Polym. Phys.* **1992**, *30*, 569.
(30) Russell, T. P. In *Handbook on Synchrotron Radiation*; Brown, G. S., Moncton, D. E., Eds.; North-Holland: New York, 1991; Vol. 3, p 379.
(31) Hiraoka, K.; Yokoyama, T. *J. Polym. Sci., Part B: Polym. Phys.* **1986**, *24*, 769.

(32) Chu, J. H.; Rangarajan, P.; Adams, J. L.; Register, R. A. *Polymer* **1995**, *36*, 1569.
(33) Taylor-Smith, R. E.; Register, R. A. *Macromolecules* **1993**, *26*, 2802.
(34) Kinning, D. J.; Thomas, E. L. *Macromolecules* **1984**, *17*, 1712.
(35) Hillmyer, M. A.; Bates, F. S.; Almdal, K.; Mortensen, K.; Ryan, A. J.; Fairclough, J. P. A. *Science* **1996**, *271*, 976.
(36) Lipic, P. M.; Bates, F. S.; Matsen, M. W. *J. Polym. Sci., Polym. Phys.* **1999**, *37*, 2229.
(37) Cohen, R. E.; Bates, F. S. *J. Polym. Sci., Polym. Phys. Ed.* **1980**, *18*, 2143.

MA020158Z